Liquid-Assisted, Etching-Free, Mechanical Peeling of 2D Materials

Yue Zhang, Qingchang liu and Baoxing Xu*

Department of Mechanical and Aerospace Engineering, University of Virginia,

Charlottesville, VA 22904, USA

Abstract

Mechanical peeling is a well-known route to transfer a single piece of two-dimensional (2D)

materials from one substrate to another one, yet heavily relies on trial and error methods. In

this work, we propose a liquid-assisted, etching-free, mechanical peeling technique of 2D

materials and systemically conduct a theoretical study of the peeling mechanics for various 2D

materials and substrates in a liquid environment. The surface wettability of 2D materials and

substrates and surface tension of liquids have been incorporated into the peeling theory to

predict the peel-off force. The theoretical model shows that the peel-off force can be

significantly affected by liquid solvents in comparison with that in dry conditions. Moreover,

our analysis reveals that the mechanical peeling-induced selective interface delamination in

multilayered 2D materials can be achieved by employing a liquid environment. These

theoretical results and demonstrations have been extensively confirmed by comprehensive

molecular dynamics simulations and good agreement is obtained between them. The present

work in theory provides a new approach of peeling 2D materials from substrates and can also

be extended for peeling thin films and membranes.

Keywords: 2D materials; mechanical peeling; surface wettability; liquid environment; theory

1. Introduction

Atomically thin two-dimensional (2D) materials, also referred to as monolayer materials, have

attracted extraordinary attention since the discovery of graphene.[1] The continuous interest of

2D materials is largely motivated by application spaces ranging from flexible electronics[2] to

high-efficiency water purification,[3] from transparent films[4] to anti-corrosion coatings, [5]

and from highly sensitive gas sensors[6] to drug delivery systems,[7] because of their

superlative properties including strength, conductivity, flexibility and transparency which are

* Corresponding author: bx4c@virginia.edu

1

beyond their bulk counterparts. To realize the myriad of these applications, the transfer of 2D materials from their growth/processed substrate to target substrate with a clean surface in a low-cost and high-yield manner is very critical.

Numbers of transfer methods have been developed over the last decades from the earliest mechanically peeling of graphene from graphite by scotch tape.[8] For instance, to isolate a single layer film from their bulk materials, through the balance of the solvent-2D material interaction in different solvents, liquid-phase mechanical exfoliation has been used to produce graphene, [9] hexagonal boron nitride, [10] transition metal dichalcogenides, [11] and layered metal oxides. [12] To transfer graphene CVD-grown on metal substrates (e.g. Fe, Ru, Co, Ni, and Cu), chemical etching of the seed metals by their etchants or electrochemical delamination of graphene and substrates have been proposed.[4, 13, 14] In the transfer of MoS₂, ultrasonication-induced microbubble in a liquid environment is developed to help delaminate the MoS₂ layers from substrate,[15] and this similar mechanical technique is also applied to roll-to-roll technique in the transfer of large-area 2D materials.[16]

From the mechanical exfoliation to environment-assisted transfer, most transfers involve the use of chemicals, sometimes with the employment of scarifying layers, in particular, in the transfer of CVD-grown 2D materials onto target substrates. In principle, the successful transfer of a film is to apply a peel-off force that leads to an energy release rate at the interface beyond the critical one, and the presence of chemicals generally decreases the critical energy release rate, thus promoting the transfer. These transfer processes inevitably lead to degradation and damage (e.g. failure or contamination) of 2D materials,[17, 18] and consumption of the substrates.[19] Generally, the adhesive interactions between most 2D materials and substrates are van der Waals force. [20-22] In comparison with a direct chemical degradation to substrates, the presence of liquid molecules will affect physical interactions at the interfaces between film and substrate and can be utilized to regulate their interfacial energy without the need of chemical etching.

In the present study, we will introduce in theory an alternative approach of transferring 2D materials in a liquid environment. This approach relies on the surface wettability of both 2D materials and substrates to liquid environments and is free of chemical reaction. A mechanics theory is proposed to quantitatively probe the effect of liquid on peel-off process by

integrating the surface wettability with classic peel-off theory and is validated by extensive molecular dynamics (MD) simulations. The peeling-induced sliding of 2D materials at the interface is also discussed. Applications in the transfer of monolayer and layered graphene-hexagonal boron nitride (h-BN) heterostructures on various substrates are demonstrated, and remarkable agreement between theoretical predictions and MD simulations is obtained.

2. Mechanics model of liquid-assisted mechanical peeling

2.1 Peeling of a monolayer 2D material

Given the weak van der Waals interaction between 2D materials and substrates, in addition to the vertical peeling from the substrates, a lateral sliding of 2D materials along the substrates may happen during the peeling process. [23] Without loss of generality, assume there is a sliding distance Δd and peeling length of Δl when a monolayer 2D material with width of b is peeled off from a substrate by a peel-off force F at the peel-off angle of α in a liquid environment, as illustrated in **Figure 1a**. Consider this peeling process is quasi-static, the energy balance among the work done by peel-off force W^F , elastic deformation of the 2D material $E_{deformation}$, and surface energy between solid and liquid $E_{surface}$ will lead to [24, 25]

$$W^F + E_{deformation} = E_{surface} \tag{1}$$

Where $W^F = F(1-cos\alpha)\Delta l + Fcos\alpha\Delta d$, and $E_{deformation} = \frac{F^2(\Delta l + \Delta d + |\Delta l - \Delta d|)}{4bEt}$, where $\frac{\Delta l + \Delta d + |\Delta l - \Delta d|}{2}$ represents the length of unadhered thin film, E and t are the Young's modulus and thickness of the monolayer 2D material, respectively. Due to the presence of liquid, we have $E_{surface} = (\gamma_{tl} + \gamma_{sl} - \gamma_{ts}) b \frac{\Delta l + \Delta d + |\Delta l - \Delta d|}{2}$, and with the help of the Young's equation $\gamma_{tl} = \gamma_t - \gamma_l cos\theta_{tl}$, $\gamma_{sl} = \gamma_s - \gamma_l cos\theta_{sl}$, we have $E_{surface} = [(\gamma_t + \gamma_s - \gamma_{ts}) - \gamma_l (cos\theta_{tl} + cos\theta_{sl})] b \frac{\Delta l + \Delta d + |\Delta l - \Delta d|}{2}$, where γ_t , γ_s and γ_t are the surface tension of 2D material, substrate and liquid, respectively. γ_{ts} , γ_{tl} and γ_{sl} are the interface tension between 2D material and substrate, 2D material and liquid, and substrate and liquid, respectively. θ_{tl} and θ_{sl} are the contact angle between 2D material and liquid, and substrate and liquid at the equilibrium, respectively, and are employed to characterize the surface wettability of 2D material and substrate, respectively. The parameter λ is the sliding factor

and is defined as $\lambda = \frac{\Delta l}{\Delta l + \Delta d}$. At $\lambda = 1$, there is no lateral sliding and only a vertical peeling of 2D material occurs; at $\lambda = 0$ there is a purely lateral sliding without vertical peeling. Therefore, the peel-off force per unit width can be written as

$$\frac{F}{b} = \frac{-2(\lambda + \cos\alpha - 2\lambda\cos\alpha)Et}{1 + |2\lambda - 1|} + \sqrt{\frac{4(Et)^2(\lambda + \cos\alpha - 2\lambda\cos\alpha)^2}{(1 + |2\lambda - 1|)^2} + 2Et[G_{ts} - \gamma_l(\cos\theta_{sl} + \cos\theta_{tl})]}$$
(2)

Where $G_{ts} = \gamma_t + \gamma_s - \gamma_{ts}$ is the interface adhesion energy between the 2D material and substrate in dry conditions.

Generally, the elastic deformation is very small during the peeling of most 2D materials such as graphene due to ultrahigh in-plane stiffness, [26, 27] and the effect of $E_{deformation}$ on the peel-off force can be neglected (See supplementary **Figure S1a** and **b**). Note that when the 2D materials possesses a low in-plane stiffness such as phosphorene, [28-30] the elastic deformation effect may become obvious (See supplementary **Figure S1c** and **d**). For simplification, with the neglectful elastic deformation, Equation (2) can be written as

$$\frac{F}{b} = \frac{1 + |2\lambda - 1|}{2(\lambda + \cos\alpha - 2\lambda\cos\alpha)} \left[G_{ts} - \gamma_l(\cos\theta_{sl} + \cos\theta_{tl}) \right] \tag{3}$$

Equation (3) shows that there is a minimum peel-off force F/b at $\alpha=0^\circ$, where the peeling distance Δl is zero, i.e. $\lambda=0$, and only lateral sliding of 2D materials along the interface occurs. Besides, when the peeling angle $0<\alpha<90^\circ$, the peel-off force reaches a minimum value at $\lambda=0.5$, where there is an equal contribution of vertical peeling and lateral sliding in the peeling of 2D materials from substrate. When the peeling angle $\alpha\geq90^\circ$, the peel-off force has the minimum value at $\lambda=1$, where there is only vertical peeling and the lateral sliding will not happen. Under this circumstance, the minimum peel-off force F/b can be summarized to

$$\left(\frac{F}{b}\right)_{min} = \begin{cases}
G_{ts} - \gamma_l(\cos\theta_{sl} + \cos\theta_{tl}), & 0^\circ \le \alpha < 90^\circ \\
\frac{1}{1 - \cos\alpha} [G_{ts} - \gamma_l(\cos\theta_{sl} + \cos\theta_{tl})], & 90^\circ \le \alpha \le 180^\circ
\end{cases}$$
(4)

Figure 1b shows the variation of peel-off force F/b with the peeling angle α at $\theta_{tl} = 30.4^{\circ}$. It is shown that there exists a lowest bound for the peel-off force with the variation of λ at any given peeling angle, which is consistent with $(F/b)_{min}$ in Equation (4). The similar results are obtained for $\theta_{tl} = 92.5^{\circ}$ and $\theta_{tl} = 151.2^{\circ}$ (Supplementary Figure S2). We should note that when the peeling is conducted in dry conditions, and the lateral sliding is not considered (i.e. $\lambda = 1$), Equation (3) will reduce to the classical Kendall's peeling model

with the peel-off force of $\frac{F_d}{b} = \frac{G_{ts}}{1 - cos\alpha}$. [24]

2.2 Peeling of multilayered 2D materials

When there are multilayered 2D materials on a substrate, the peel-off force required to peel a certain number of layers can also be obtained by following a similar procedure with that of a monolayer in Section 2.1. Because the minimum peel-off force is desirable in practical experiments, the minimum peel-off force in this section will be focused. Assume n layers $(1 \le n \le N, N)$ is the total number of layers on substrate) need to be peeled off, the n layers can be considered an integrated one and the rest layers and substrate is deemed a new substrate. Under this assumption, similar to Equations (2) and (4), the minimum peel-off force can be obtained via

$$(\frac{F}{b})_{min} = \begin{cases} \frac{-1 + \sqrt{2(\frac{1}{t_1 E_1} + \frac{1}{t_2 E_2} + \dots + \frac{1}{t_n E_n})[c_{tn-tn+1} - \gamma_l(\cos\theta_{tln} + \cos\theta_{tln+1})]}}{\frac{1}{t_1 E_1} + \frac{1}{t_2 E_2} + \dots + \frac{1}{t_n E_n}}}, & 0^{\circ} \le \alpha < 90^{\circ} \\ \frac{-(1 - \cos\alpha) + \sqrt{(1 - \cos\alpha)^2 + 2(\frac{1}{t_1 E_1} + \frac{1}{t_2 E_2} + \dots + \frac{1}{t_n E_n})[c_{tn-tn+1} - \gamma_l(\cos\theta_{tln} + \cos\theta_{tln+1})]}}{\frac{1}{t_1 E_1} + \frac{1}{t_2 E_2} + \dots + \frac{1}{t_n E_n}}}, & at 1 \le n \le N - \end{cases}$$

1 (5)

and when n = N, all layers will be considered an integrated one and the separation will occur at the interface between the bottommost layer and substrate, and the minimum peel-off force will be

$$(\frac{F}{b})_{min} = \begin{cases} \frac{-1 + \sqrt{2(\frac{1}{t_1 E_1} + \frac{1}{t_2 E_2} + \dots + \frac{1}{t_N E_N})[G_{tN-s} - \gamma_l(\cos\theta_{tlN} + \cos\theta_{sl})]}}{\frac{1}{t_1 E_1} + \frac{1}{t_2 E_2} + \dots + \frac{1}{t_N E_N}}, & 0^{\circ} \leq \alpha < 90^{\circ} \\ \frac{-(1 - \cos\alpha) + \sqrt{(1 - \cos\alpha)^2 + 2(\frac{1}{t_1 E_1} + \frac{1}{t_2 E_2} + \dots + \frac{1}{t_N E_N})[G_{tN-s} - \gamma_l(\cos\theta_{tlN} + \cos\theta_{sl})]}}{\frac{1}{t_1 E_1} + \frac{1}{t_2 E_2} + \dots + \frac{1}{t_N E_N}}, & 90^{\circ} \leq \alpha \leq 180^{\circ} \end{cases}$$
 at $n = N$

(6)

where t_n and E_n (n=1,2,...N) are thickness and Young's modulus of the n^{th} layer, respectively. $G_{tn-tn+1}$ and G_{tN-s} represent the adhesion energy between n^{th} layer and $(n+1)^{th}$ layer, between N^{th} layer and substrate in dry conditions, respectively. θ_{tln} , θ_{tln+1} and θ_{sl} are the contact angle at the equilibrium and reflect surface wettability of the n^{th} , $(n+1)^{th}$ layer, and substrate in liquid, respectively.

Similar to that of monolayer, when the effect of elastic deformation can be neglected, Equations (5) and (6) will be simplified to

$$(\frac{F}{b})_{min} = \begin{cases} G_{tn-tn+1} - \gamma_l(\cos\theta_{tln} + \cos\theta_{tln+1}), & 0^{\circ} \le \alpha < 90^{\circ} \\ \frac{1}{1 - \cos\alpha} [G_{tn-tn+1} - \gamma_l(\cos\theta_{tln} + \cos\theta_{tln+1})], & 90^{\circ} \le \alpha \le 180^{\circ} \end{cases}$$
 at $1 \le n \le N$

and

$$(\frac{F}{b})_{min} = \begin{cases} G_{tN-s} - \gamma_l(\cos\theta_{tlN} + \cos\theta_{sl}), & 0^{\circ} \le \alpha < 90^{\circ} \\ \frac{1}{1 - \cos\alpha} [G_{tN-s} - \gamma_l(\cos\theta_{tlN} + \cos\theta_{sl})], & 90^{\circ} \le \alpha \le 180^{\circ} \end{cases}$$
 at $n = N$ (8)

Further, when these N layers are the same in materials such as graphite, Equations (7) and (8) will reduce to

$$(\frac{F}{b})_{min} = \begin{cases} G_{tt} - 2\gamma_l cos\theta_{tl}, & 0^{\circ} \le \alpha < 90^{\circ} \\ \frac{1}{1 - cos\alpha} (G_{tt} - 2\gamma_l cos\theta_{tl}), & 90^{\circ} \le \alpha \le 180^{\circ} \end{cases}$$
 at $1 \le n \le N - 1$ (9)

and

$$(\frac{F}{b})_{min} = \begin{cases} G_{ts} - \gamma_l(\cos\theta_{tl} + \cos\theta_{sl}), & 0^{\circ} \le \alpha < 90^{\circ} \\ \frac{1}{1 - \cos\alpha} [G_{ts} - \gamma_l(\cos\theta_{tl} + \cos\theta_{sl})], & 90^{\circ} \le \alpha \le 180^{\circ} \end{cases}$$
 at $n = N$ (10)

Where G_{tt} represents the adhesion energy between monolayers in dry conditions.

Equation (9) indicates that $(F/b)_{min}$ is always the same at each interface when the layers are the same 2D material, which echoes the randomness of peeling of graphene from graphite by scotch tape. [8] When materials for layers are different, Equations (7) and (8) show that $(F/b)_{min}$ will be different, and the presence of liquid may facilitate or resist the peeling of them together or individuals. We should note that when peeling off films in macroscopic scale with a low elastic modulus such as soft membranes,[24] or functionally graded composites with different materials or thickness in each layer,[31] the peel-off event along a desirable interface is possible because the effect of elastic term cannot be neglected, and Equations (5) and (6) should be used.

As a theoretical demonstration, **Figure 2a** illustrates a peeling of two layered 2D materials from a substrate in liquid under a peel-off force applied on the top layer (layer 1). As we analyze above, two resultant situations could happen. In situation (I), only top layer 1 is peeled off and layer 2 remains a perfect adhesive on substrate, where the corresponding minimum peeling-off force obtained via Equation (7) is referred to as $F_{\rm I}$ and $F_{\rm wI}$ in dry condition and liquid environment, respectively. In situation (II), both layers 1 and 2 are peeled off together from substrate, and the corresponding minimum peeling force obtained via Equation (8) is referred

to as F_{II} and F_{wII} in dry condition and liquid environment, respectively. Figure 2b and c shows the comparison of the peel-off force between these two situations in both dry condition and liquid environment. In dry air condition, the relation between $F_{\rm I}$ and $F_{\rm II}$ only depends on the difference of interface adhesion energy $G_{t2-s}-G_{t1-t2}$, where G_{t1-t2} denotes the adhesion energy at the interface between layer 1 and the layer 2 in dry condition, and G_{t2-s} denotes the adhesion energy at the interface between the layer 2 and substrate in dry condition. When $G_{t2-s}-G_{t1-t2}>0$, $F_{\rm II}>F_{\rm I}$ and when $G_{t2-s}-G_{t1-t2}<0$, $F_{\rm II}< F_{\rm I}$. In contrast, in liquid environments, the relation between F_{wI} and F_{wII} depend on not only $G_{t2-s} - G_{t1-t2}$ but also θ_{tl1} and θ_{sl} , where θ_{tl1} and θ_{sl} represent the contact angle of the layer 1 and substrate in liquid at the equilibrium, respectively. For example, as shown in Figure 2b, for the substrate with a high surface wettability (i.e. a small θ_{sl}), F_{wll} could become lower than F_{wI} even though $G_{t2-s} - G_{t1-t2} > 0$, and if θ_{sl} is large enough, $F_{wII} > 0$ F_{wl} could also be obtained at $G_{t2-s} - G_{t1-t2} < 0$. Similarly, when the layer 1 possesses a high surface wettability (i.e. small θ_{tl1}), Figure 2c shows that F_{wl} is less than F_{wll} even at $G_{t2-s} - G_{t1-t2} < 0$ and at a higher θ_{tl1} , $F_{wI} > F_{wII}$ is obtained. These differences of peel-off force between in dry and liquid conditions show that the liquid environment can be leveraged to achieve the peeling of 2D materials with a desirable number of layers separation from substrate by carefully controlling the surface wettability, as summarized in **Supplementary Figure S3.**

3. Computational modeling and method

All the MD simulations were carried out using the Large-scale Atomic/Molecular Massively Parallel Simulator (LAMMPS) package.[32] Two typical 2D materials, graphene and hexagonal boron nitride (h-BN) with width of 2 nm and length of 6 nm, were employed as representatives. The graphene, copper and silicon were chosen as representatives of substrates. The adaptive intermolecular reactive bond order (AIREBO) [33, 34] and Stillinger-Weber (SW) potentials[35] were employed to model the flexible graphene and h-BN respectively because these potentials have proved to reproduce their mechanical properties. The popular embedded atom potential [36] and Tersoff potential [37] were utilized to model the copper and silicon materials, respectively. The 2D materials were placed on the top surface of substrate and

immersed in a liquid water environment. The size of water liquid box was 4 nm \times 10 nm \times 6 nm which is sufficiently large to ensure a full immersion of 2D materials and substrate during the entire peel-off process. The water molecules were modeled using the extended simple point charge (SPC/E) model.[38] The non-bonded interaction among 2D materials, liquid and substrate were modeled by the 12-6 pairwise Lennard-Jones potential $V(r) = 4\varepsilon(\sigma^{12}/r^{12} - \sigma^6/r^6)$ and Coulomb interaction $V_q(r) = q_i q_j / 4\pi\varepsilon_0 r$, where σ and ε are the equilibrium distance and the interactive well depth of the potential, respectively, r is the interatomic distance, and q_i and q_j are the electronic charge counterpart, and ε_0 is the permittivity of vacuum. The cut-off radius was chosen 1.0 nm for all L-J interactions to calculate the short-range van der Waals forces, and the particle-particle-particle-mesh (PPPM) algorithm with a root mean of 0.0001 was used to handle the long range Coulomb interactions. The contact angle θ of water droplet on the surface of 2D materials or substrate at the equilibrium is used to characterize their surface wettability. In addition, the interactive well depth ε was tuned in the simulations to achieve different surface wettability of graphene, which has proved to well mimic chemical surface treatments in experiments. [39-41]

In the simulation of peeling of 2D materials from substrate, we first carried out equilibrium simulations through relaxation and thermalization of the system to 300 K with a time step of 1.0 fs for 0.5 ns. After that, the steered molecular dynamics method was used to peel off the 2D materials. Specifically, we clamped atoms at one edge of the topmost layer 2D materials by constraining their relative positions. The clamped atoms were connected with one end of a spring and the other end of the spring was applied by a displacement loading with a peeling angle α . The loading rate was v = 0.01Å/ps and proves to mimic a quasi-static loading. The spring stiffness was k = 0.1eV/Å, which is at the same level with the stiffness of AFM cantilever.[42] The bottom atoms of substrate were fixed in the simulations. Unless otherwise stated, all simulations were performed in NVT ensemble with Nose/Hoover thermostat at temperature 300 K. In parallel, the quasi-static peel-off simulations in dry conditions were also performed for comparison. During all the simulations, potential energy between 2D material layers, substrate and water molecules and positions of all the atoms in the system were monitored every 10000 steps with a time step of 1.0 fs to ensure the sufficient data

recorded in analysis.

4. Results and discussions

We first conducted simulations on the peeling of a single layer flexible graphene on a substrate in both dry condition and water environments. **Figure 3a** shows the variation of peel-off force with simulation time at the peeling angle $\alpha = 90^{\circ}$, where the substrate is graphene with the surface wettability of $\theta_{sl} = 95.0^{\circ}$ in water. Independent of peel-off environments and surface wettability of graphene layer, all peel-off forces increase quickly at the beginning and reach a maximum value, and then decrease till to arriving at a steady state with a constant magnitude (snapshots see **Supplementary Figure S4a**). More importantly, when the graphene film to be peeled is hydrophilic with $\theta_{tl} = 30.4^{\circ}$, the peel-off force at the steady state is lower in water environment than that in dry condition. In contrast, if the graphene film is hydrophobic with $\theta_{tl} = 151.2^{\circ}$, the peel-off force at the steady state is higher in water environment than that in dry condition. This opposite effect of water on peel-off force indicates the importance of surface wettability of graphene layer.

Further, by taking the peel-off force at the steady state, we calculate the difference of the peel-off force between in water environment and in dry condition $\Delta F/b$ as the variation of contact angle of graphene layer θ_{tl} , and plot them in **Figure 3b**. $\Delta F/b$ shows a monotonous increase with the increase of θ_{tl} . In parallel, given these parameters, the theoretical plots of $\Delta F/b$ as a function of θ_{tl} can be obtained by using Equation (4) and are also given in **Figure 3b** for comparison, where the surface tension of water is $\gamma_l = 61.3 \times 10^{-3} N/m$ [43, 44]. Good agreement between MD simulations and theoretical results are observed. Besides, it is shown that $\Delta F/b = 0$ at $\theta_{tl} = 85.0^{\circ}$. When $\theta_{tl} < 85.0^{\circ}$, $\Delta F/b < 0$, indicating that the presence of water will promote the peeling of 2D materials from a graphene substrate; if the 2D materials have a surface wettability with $\theta_{tl} > 85.0^{\circ}$, the water environment will lead to resistance to its successful peeling from graphene substrate. In addition, at a given θ_{tl} , when the substrate changes, the monotonous variation of $\Delta F/b$ with θ_{tl} is also obtained, and $\Delta F/b$ will increase with the increase of θ_{sl} . For example, when the graphene is peeled from the silicon substrate which has a lower wettability ($\theta_{sl} = 110.6^{\circ}$) than that of graphene substrate ($\theta_{sl} = 95.0^{\circ}$), a higher $\Delta F/b$ is obtained, and by contrast, a lower $\Delta F/b$ is

obtained to peel off the graphene from copper substrate ($\theta_{sl} = 60.9^{\circ}$) in comparison with that from graphene substrate because of higher wettability. These theoretical plots are also well consistent with MD simulations. When the liquid solvent changes, a similar variation of $\Delta F/b$ with θ_{tl} is obtained because of dependence of peel-off force on surface tension of liquid γ_l , as indicated in Equation (4). Both theoretical plots and MD simulations are given in **Supplementary Figure S5** and their good agreement is also obtained. In essence, our theoretical analysis indicates the presence of liquid will lead to a change of adhesion energy between 2D layer and environment when it is peeled from substrate. **Figure S4b** presents the interfacial energy difference of peeling 2D graphene layer from graphene substrate in liquid water in comparison with that in dry condition, which corresponds to plots in Figure 3a. For a graphene layer with $\theta_{tl} = 30.4^{\circ}$, it is shown that the graphene layer has a lower interfacial energy than that in dry condition, which agrees with a lower peel-off force in water than that in dry condition. In contrast, for a graphene layer with $\theta_{tl} = 151.2^{\circ}$, the graphene layer has a higher interfacial energy than that in dry condition, which is also in good consistency with a higher peel-off force in water than that in dry condition.

Figure 4a shows the peel-off force of graphene F/b in water environment with $\theta_{tl} = 30.4^{\circ}$ and $\theta_{sl} = 95.0^{\circ}$. Similar to observations in Figure 3a, the peel-off force reaches a steady state after the initial adjustment. Besides, the peel-off force at the steady state at the peeling angle $\alpha = 120^{\circ}$ is smaller than that of $\alpha \le 90^{\circ}$. More importantly, when $\alpha \le 90^{\circ}$, the peel-off force at the steady state is approximately the same and does not change with α , which is in good consistency with theoretical analysis in Equation (4). Figure 4b shows quantitative comparison of the minimum peel-off force in water $(F/b)_{min}$ between MD simulations and theoretical calculations at different α and θ_{tl} , where the interlayer adhesion energy of graphene is taken as $G_{ts} = 1.45 eV/nm^2$ in the theoretical calculations via Equation (4).[45-47] Remarkable consistency between them is obtained. Besides, at the same α , a higher θ_{tl} will lead to a higher $(F/b)_{min}$. Figure S6a presents the MD snapshots at different simulation times. Only a lateral sliding of graphene layer on substrate at $\alpha = 0^{\circ}$ is observed, both lateral sliding and vertical peeling occur at $\alpha = 45^{\circ}$, and only vertical peeling occurs at $\alpha = 90^{\circ}$, which agrees well with theoretical analysis. In addition, different from these peel-off behaviors, once the peel-off force arrives at the steady state, the interfacial adhesion energy

difference of the 2D layer between that in water environment and in dry condition shows almost the same, independent of α , as shown in **Figure S6b**, which is also well consistent with a constant peel-off force in both theory and MD simulations in Figure 4b.

When there are two layered 2D materials on the substrate, the theoretical analysis (Figure 2, or Equations (7) and (8)) shows that the liquid environment could change the peel-off forces at different separation interfaces, and can be utilized to control the separation at a desirable interface. As a numerical demonstration, we performed MD simulations by employing graphene and h-BN as 2D materials and copper and silicon as substrate. Note that the load was always applied to the topmost layer for all simulations so as to ensure practical applications of these demonstrations in experiments. Figure 5a shows MD snapshots of peeling two layered graphene from copper substrate with the pee-off angle of $\alpha = 45^{\circ}$. Their peel-off force with simulation time is shown in Figure S7. In the dry condition, the top layered graphene is detached with the increase of peel-off time, and the bottom layered graphene stays on the substrate. In contrast, when the peeling is conducted in the water liquid, both graphene layers are delaminated from substrate. When the copper substrate is replaced by silicon (Figure 5b), in dry condition, both graphene layers are detached; and in water environment, only the top graphene layer is peeled of, which is completely different from the separation event on copper substrate. In theory, when two layered graphene sheets are placed on copper substrate, because $G_{t2-s} = 1.62 \text{eV/nm}^2$,[26] and $G_{t1-t2} = 1.45 \text{eV/nm}^2$,[46] binding energy and $G_{t2-s} - G_{t1-t2} > 0$, and given $\theta_{tl1} = 95.0^{\circ}$ and $\theta_{sl} = 60.9^{\circ}$, we will have $F_{II} > F_{I}$ from the peel-off map in Figure 2b in the dry condition, and thus the separation tends to occur at the interface between two graphene layers; Similarly, in water environment, we have F_{wII} < F_{wI} , leading to a separation of both graphene layers from copper substrate, which is in good consistency with MD simulations. When the substrate changes to silicon, the consistency between MD simulations and theoretical predictions can be confirmed through comparison of interface adhesion energy among graphene, graphene and silicon substrate and surface wettability of graphene and silicon. Further, when peeling off two different layered 2D materials, graphene and h-BN from copper substrate, because $G_{t2-s} = 1.62 \text{eV/nm}^2$, and $G_{t1-t2} = 1.69 \text{eV/nm}^2, [48] \text{ and } \quad G_{t2-s} - G_{t1-t2} < 0, \text{ and } \quad \theta_{tl1} = 29.7^\circ \text{ and } \quad \theta_{sl} = 60.9^\circ,$

the theoretical calculations based on Figure 2c predict that in the dry condition, $F_{II} < F_{I}$, and the separation tends to occur between graphene and substrate; and in water environment, $F_{wII} > F_{wI}$, and the separation tends to occur between graphene and boron nitride, which is also in good consistency with MD simulations in **Figure 5c**.

5. Conclusion

By introducing a liquid environment to the conventional mechanical peeling experiments, we propose a liquid-assisted peeling technique capable of peeling of 2D materials from substrates without chemical reaction involved. A physical mechanics model that integrates the peel-off force and angle with surface wettability of 2D materials and substrates, surface tension of liquid, and interfacial energy between 2D materials and substrates in dry conditions is developed and utilized to predict the peeling phenomena of 2D materials from various substrates. When peeling off a single layer 2D materials from a substrate, the theoretical analysis shows if 2D materials and substrate are both hydrophilic, the presence of liquid molecules will lead to a lower peel-off force in comparison with that in dry conditions, and promotes the interfacial peeling. Moreover, the theory is extended to the peeling of multilayered 2D material system, and an explicit peel-off force in liquid is also given. In particular, the analysis on peeling of two layered 2D materials indicates that the interfacial separation can be completely different in between a liquid environment and dry condition. The extensive molecular dynamics simulations were performed and the results show remarkable consistency with theoretical predictions.

The present study is expected to provide an immediate guidance for mechanical peeling and transferring of 2D materials from various growth substrates to target substrates to meet the needs in the fabrication of 2D materials enabled devices, where the liquid could be employed to tune the peel-off force and achieve the selective delamination at a desirable interface. Further, with the inherent van der Waals force interaction between films and substrates, it is envisioned that our theoretical model can also be used in macroscale device fabrications that rely on transfer printing process. Moreover, this study may facilitate the other manufacturing techniques of 2D materials by employing a proper liquid solvents such as the popular mechanical exfoliation in solvents.

Acknowledgment:

This work is supported by the University of Virginia and NSFCMMI-1728149.

References:

- [1] Akinwande D, Brennan CJ, Bunch JS, Egberts P, Felts JR, Gao H, Huang R, Kim J-S, Li T, Li Y. A review on mechanics and mechanical properties of 2D materials—Graphene and beyond. Extreme Mechanics Letters 2017.
- [2] Georgiou T, Jalil R, Belle BD, Britnell L, Gorbachev RV, Morozov SV, Kim Y-J, Gholinia A, Haigh SJ, Makarovsky O. Vertical field-effect transistor based on graphene-WS2 heterostructures for flexible and transparent electronics. Nature nanotechnology 2013;8:100.
- [3] Han Y, Xu Z, Gao C. Ultrathin graphene nanofiltration membrane for water purification. Advanced Functional Materials 2013;23:3693.
- [4] Bae S, Kim H, Lee Y, Xu X, Park J-S, Zheng Y, Balakrishnan J, Lei T, Kim HR, Song YI. Roll-to-roll production of 30-inch graphene films for transparent electrodes. Nature nanotechnology 2010;5:574.
- [5] Chang C-H, Huang T-C, Peng C-W, Yeh T-C, Lu H-I, Hung W-I, Weng C-J, Yang T-I, Yeh J-M. Novel anticorrosion coatings prepared from polyaniline/graphene composites. Carbon 2012;50:5044.
- [6] Li W, Geng X, Guo Y, Rong J, Gong Y, Wu L, Zhang X, Li P, Xu J, Cheng G. Reduced graphene oxide electrically contacted graphene sensor for highly sensitive nitric oxide detection. ACS nano 2011;5:6955.
- [7] Liu J, Cui L, Losic D. Graphene and graphene oxide as new nanocarriers for drug delivery applications. Acta biomaterialia 2013;9:9243.
- [8] Novoselov KS, Geim AK, Morozov SV, Jiang D, Zhang Y, Dubonos SV, Grigorieva IV, Firsov AA. Electric field effect in atomically thin carbon films. science 2004;306:666.
- [9] Hernandez Y, Nicolosi V, Lotya M, Blighe FM, Sun Z, De S, McGovern I, Holland B, Byrne M, Gun'Ko YK. High-yield production of graphene by liquid-phase exfoliation of graphite. Nature nanotechnology 2008;3:563.
- [10] Zhi C, Bando Y, Tang C, Kuwahara H, Golberg D. Large-scale fabrication of boron nitride nanosheets and their utilization in polymeric composites with improved thermal and mechanical properties. Advanced Materials 2009;21:2889.
- [11] Coleman JN, Lotya M, O'Neill A, Bergin SD, King PJ, Khan U, Young K, Gaucher A, De S, Smith RJ. Two-dimensional nanosheets produced by liquid exfoliation of layered materials. Science 2011;331:568.
- [12] Dias AS, Lima S, Carriazo D, Rives V, Pillinger M, Valente AA. Exfoliated titanate, niobate and titanoniobate nanosheets as solid acid catalysts for the liquid-phase dehydration of D-xylose into furfural. Journal of Catalysis 2006;244:230.
- [13] Li X, Zhu Y, Cai W, Borysiak M, Han B, Chen D, Piner RD, Colombo L, Ruoff RS. Transfer of large-area graphene films for high-performance transparent conductive electrodes. Nano letters 2009;9:4359.
- [14] Regan W, Alem N, Alemán B, Geng B, Girit Ç, Maserati L, Wang F, Crommie M, Zettl A. A direct transfer of layer-area graphene. Applied Physics Letters 2010;96:113102.
- [15] Ma D, Shi J, Ji Q, Chen K, Yin J, Lin Y, Zhang Y, Liu M, Feng Q, Song X. A universal etching-free transfer of MoS2 films for applications in photodetectors. Nano Research

- 2015;8:3662.
- [16] Kobayashi T, Bando M, Kimura N, Shimizu K, Kadono K, Umezu N, Miyahara K, Hayazaki S, Nagai S, Mizuguchi Y. Production of a 100-m-long high-quality graphene transparent conductive film by roll-to-roll chemical vapor deposition and transfer process. Applied Physics Letters 2013;102:023112.
- [17] Pirkle A, Chan J, Venugopal A, Hinojos D, Magnuson C, McDonnell S, Colombo L, Vogel E, Ruoff R, Wallace R. The effect of chemical residues on the physical and electrical properties of chemical vapor deposited graphene transferred to SiO2. Applied Physics Letters 2011;99:122108.
- [18] Suk JW, Kitt A, Magnuson CW, Hao Y, Ahmed S, An J, Swan AK, Goldberg BB, Ruoff RS. Transfer of CVD-grown monolayer graphene onto arbitrary substrates. ACS nano 2011;5:6916.
- [19] Mahenderkar NK, Chen Q, Liu Y-C, Duchild AR, Hofheins S, Chason E, Switzer JA. Epitaxial lift-off of electrodeposited single-crystal gold foils for flexible electronics. Science 2017;355:1203.
- [20] Ishigami M, Chen J, Cullen W, Fuhrer M, Williams E. Atomic structure of graphene on SiO2. Nano letters 2007;7:1643.
- [21] Koenig SP, Boddeti NG, Dunn ML, Bunch JS. Ultrastrong adhesion of graphene membranes. Nature nanotechnology 2011;6:543.
- [22] Boddeti NG, Liu X, Long R, Xiao J, Bunch JS, Dunn ML. Graphene blisters with switchable shapes controlled by pressure and adhesion. Nano letters 2013;13:6216.
- [23] Feng X, Kwon S, Park JY, Salmeron M. Superlubric sliding of graphene nanoflakes on graphene. ACS nano 2013;7:1718.
- [24] Kendall K. Thin-film peeling-the elastic term. Journal of Physics D: Applied Physics 1975;8:1449.
- [25] Kim K-S, Kim J. Elasto-plastic analysis of the peel test for thin film adhesion. Journal of Engineering Materials and Technology 1988;110:266.
- [26] Shi X, Yin Q, Wei Y. A theoretical analysis of the surface dependent binding, peeling and folding of graphene on single crystal copper. Carbon 2012;50:3055.
- [27] Gao Y, Liu Q, Xu B. Lattice Mismatch Dominant Yet Mechanically Tunable Thermal Conductivity in Bilayer Heterostructures. Acs Nano 2016;10:5431.
- [28] Jiang J-W, Park HS. Mechanical properties of single-layer black phosphorus. Journal of Physics D: Applied Physics 2014;47:385304.
- [29] Liu N, Hong J, Pidaparti R, Wang X. Fracture patterns and the energy release rate of phosphorene. Nanoscale 2016;8:5728.
- [30] Liu N, Hong J, Zeng X, Pidaparti R, Wang X. Fracture mechanisms in multilayer phosphorene assemblies: from brittle to ductile. Physical Chemistry Chemical Physics 2017.
- [31] Erdogan F. Fracture mechanics of functionally graded materials. Composites Engineering 1995;5:753.
- [32] Plimpton S, Crozier P, Thompson A. LAMMPS-large-scale atomic/molecular massively parallel simulator. Sandia National Laboratories 2007;18.
- [33] Stuart SJ, Tutein AB, Harrison JA. A reactive potential for hydrocarbons with intermolecular interactions. The Journal of chemical physics 2000;112:6472.
- [34] Brenner DW, Shenderova OA, Harrison JA, Stuart SJ, Ni B, Sinnott SB. A second-

- generation reactive empirical bond order (REBO) potential energy expression for hydrocarbons. Journal of Physics: Condensed Matter 2002;14:783.
- [35] Moon WH, Hwang HJ. A modified Stillinger—Weber empirical potential for boron nitride. Applied surface science 2005;239:376.
- [36] Foiles S, Baskes M, Daw M. Embedded-atom-method functions for the fcc metals Cu, Ag, Au, Ni, Pd, Pt, and their alloys. Physical Review B 1986;33:7983.
- [37] Tersoff J. Empirical interatomic potential for silicon with improved elastic properties. Physical Review B 1988;38:9902.
- [38] Mark P, Nilsson L. Structure and dynamics of the TIP3P, SPC, and SPC/E water models at 298 K. The Journal of Physical Chemistry A 2001;105:9954.
- [39] Zhang Z, Li T. Carbon nanotube initiated formation of carbon nanoscrolls. Applied Physics Letters 2010;97:081909.
- [40] Liu Q, Xu B. Actuating Water Droplets on Graphene via Surface Wettability Gradients. Langmuir 2015;31:9070.
- [41] Liu Q, Xu B. A unified mechanics model of wettability gradient-driven motion of water droplet on solid surfaces. Extreme Mechanics Letters 2016;9:304.
- [42] Jiang W-G, Peng D-F, Feng X-Q. Steered Molecular Dynamics Simulations on the Peeling and Shearing of Carbon Nanotubes on a Silicon Substrate. Journal of nanoscience and nanotechnology 2013;13:5374.
- [43] Guo Y, Guo W, Chen C. Modifying atomic-scale friction between two graphene sheets: A molecular-force-field study. Physical Review B 2007;76.
- [44] Vega C, De Miguel E. Surface tension of the most popular models of water by using the test-area simulation method. The Journal of chemical physics 2007;126:154707.
- [45] Girifalco L, Hodak M, Lee RS. Carbon nanotubes, buckyballs, ropes, and a universal graphitic potential. Physical Review B 2000;62:13104.
- [46] Meng X, Li M, Kang Z, Zhang X, Xiao J. Mechanics of self-folding of single-layer graphene. Journal of Physics D: Applied Physics 2013;46:055308.
- [47]Zhang J, Xiao J, Meng X, Monroe C, Huang Y, Zuo J-M. Free folding of suspended graphene sheets by random mechanical stimulation. Physical review letters 2010;104:166805. [48]Ye Z, Otero-De-La-Roza A, Johnson ER, Martini A. Oscillatory motion in layered materials: graphene, boron nitride, and molybdenum disulfide. Nanotechnology 2015;26:165701.

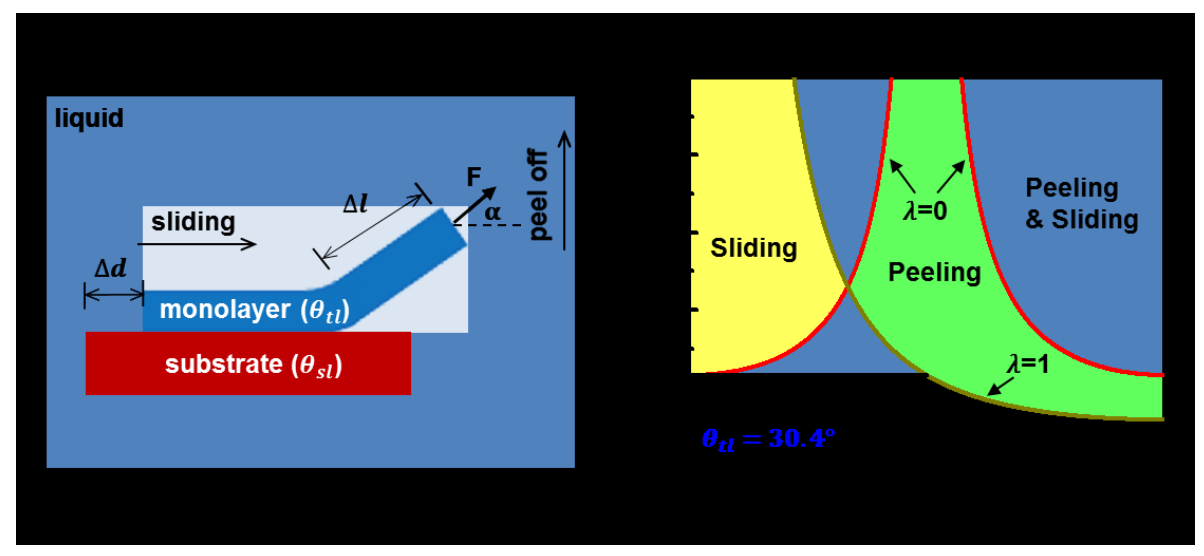


Figure 1. Peeling of a monolayer material from substrate in a liquid environment. (a) Schematic illustration of peeling of a monolayer film in liquid with both lateral sliding and vertical separation at the interface by a peel-off force F at a peeling angle α . θ_{tl} and θ_{sl} are contact angle of monolayer material and substrate in liquid at the equilibrium, respectively, and represent their surface wettability. Δd and Δl are sliding and peel-off length, respectively. (b) Peel-off force per unit width F/b of a single layer material from substrate versus peeling angle α . In the plots, the interlayer adhesion energy is $G_{ts} = 1.45 \text{eV}/nm^2$, surface tension of liquid is $\gamma_l = 61.3 \times 10^{-3} N/m$, contact angle is $\theta_{tl} = 30.4^{\circ}$ and $\theta_{sl} = 95.0^{\circ}$. Yellow region: only lateral sliding occurs, Dark blue region: both vertical peeling and lateral sliding occur, Green region: only vertical peeling occurs, and NA: neither vertical peeling nor lateral sliding occurs. λ is the sliding factor and is defined as $\lambda =$

 $\frac{\Delta l}{\Delta l + \Delta d}$.

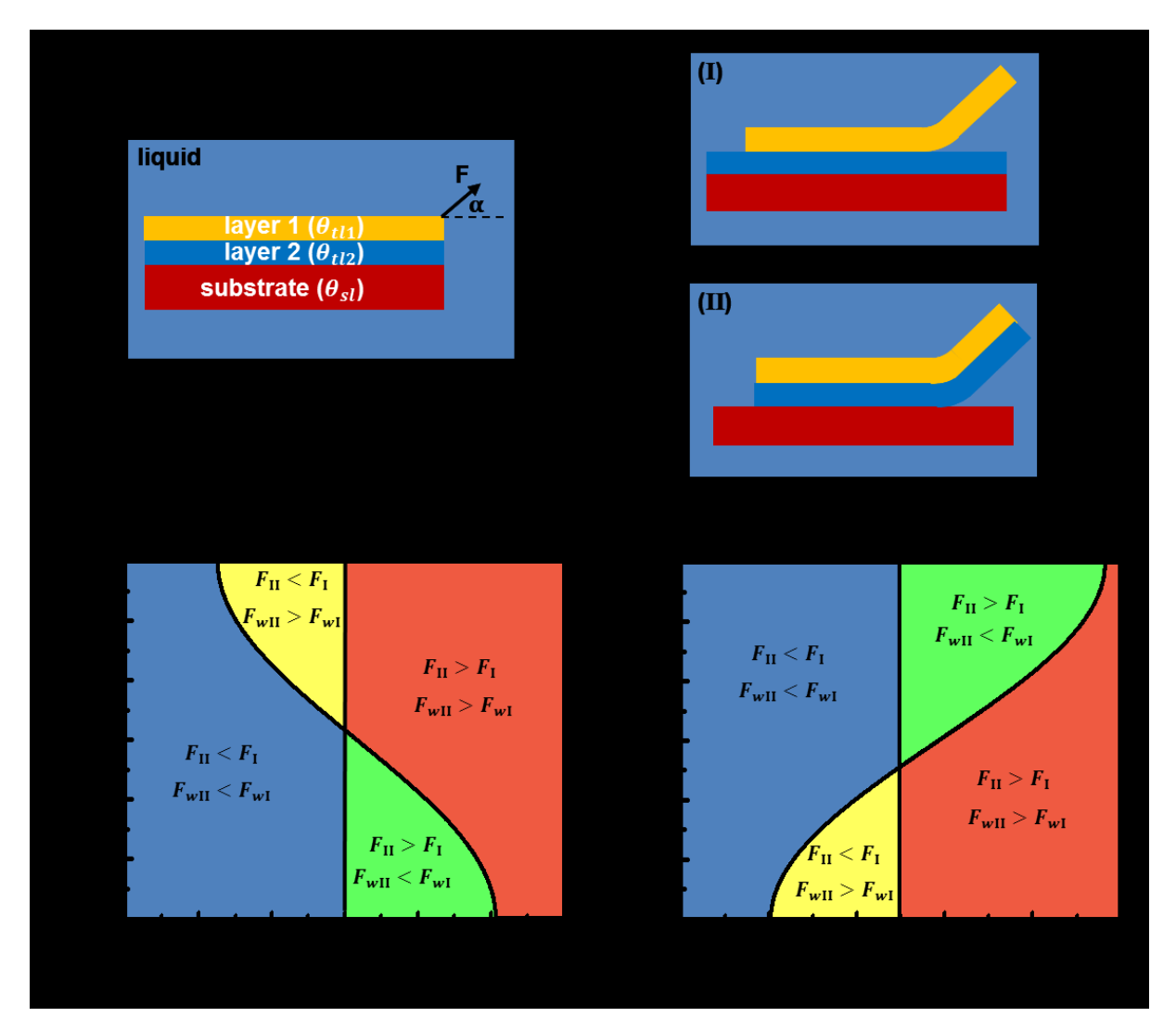


Figure 2. Peeling of a two-layered material from substrate in a liquid environment. (a) Schematic illustration of peeling of two-layer materials from a substrate by applying a peel-off force on the top layer 1 (left), and the resultant two situations (right)- (I) only top layer 1 is peeled of and layer 2 keeps adhesive on substrate and (II) both layers 1 and 2 are peeled of together from substrate. θ_{tl1} , θ_{tl2} and θ_{sl} reflect the surface wettability of layer 1 and 2, and substrate in liquid, respectively. Theoretical map of the peel-off force with variation of surface wettability of (b) substrate θ_{sl} and (c) top layer film θ_{tl1} . $G_{t2-s} - G_{t1-t2}$ is the energy difference between layer/substrate and layer/layer in adhesion condition. $F_{\rm I}$ and $F_{\rm II}$ are the minimum force of peeling of one single layer (situation I) and two layers (situation II) from substrate in dry condition, respectively, and F_{wI} and F_{wII} the minimum force of peeling of one single layer (situation I) and two layers (situation II) from substrate in liquid environments, respectively. Blue region: $F_{II} < F_{I}$ and $F_{wII} < F_{wI}$; red region: $F_{II} > F_{I}$ and $F_{wII} > F_{wI}$, and both regions indicate that the presence of liquid water will not change the peel-off position. Yellow region: $F_{\rm II} < F_{\rm I}$ and $F_{w \rm II} > F_{w \rm I}$; green region: $F_{II} > F_{I}$ and $F_{wII} < F_{wI}$, and both regions indicate that the presence of liquid water will change the peel-off position.

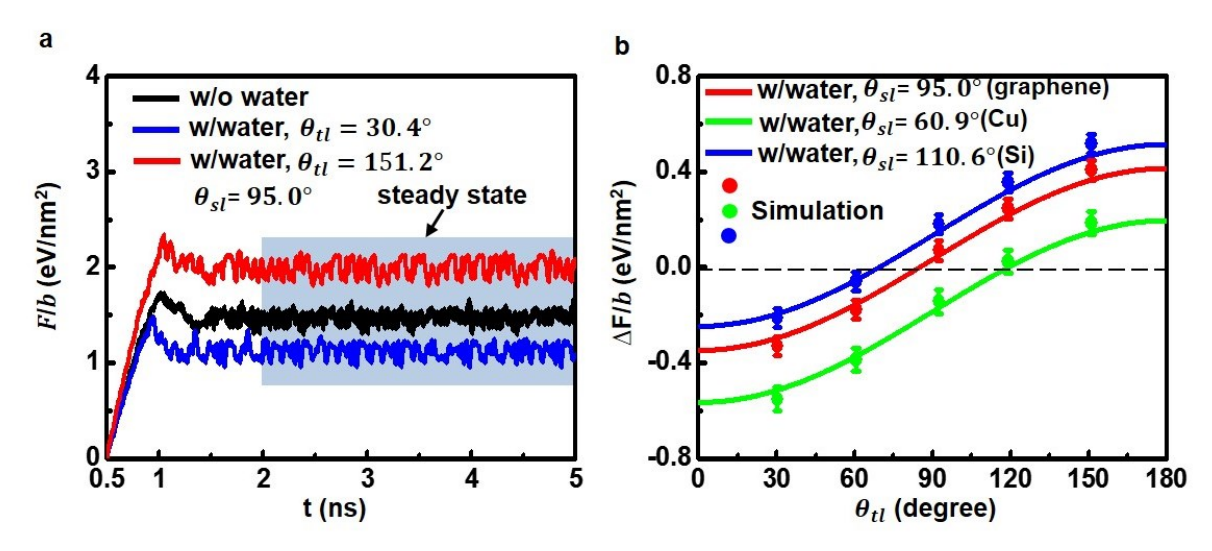


Figure 3. Variation of peel-off force of peeling of a monolayer material with different surface wettability at peeling angle $\alpha = 90^{\circ}$. (a) Comparison of peel-off force F/b in dry condition and water environment with different surface wettability of graphene θ_{tl} . The surface wettability of substrate in water is $\theta_{sl} = 95.0^{\circ}$. The peel-off force remains approximately constant in steady state (the dark boxed area). (b) MD simulation and theoretical comparison of peel-off force variation $\Delta F/b$ at the steady state of peeling of graphene with different surface wettability θ_{tl} in dry condition and water environment from different substrates θ_{sl} (copper: Cu, and silicon: Si).

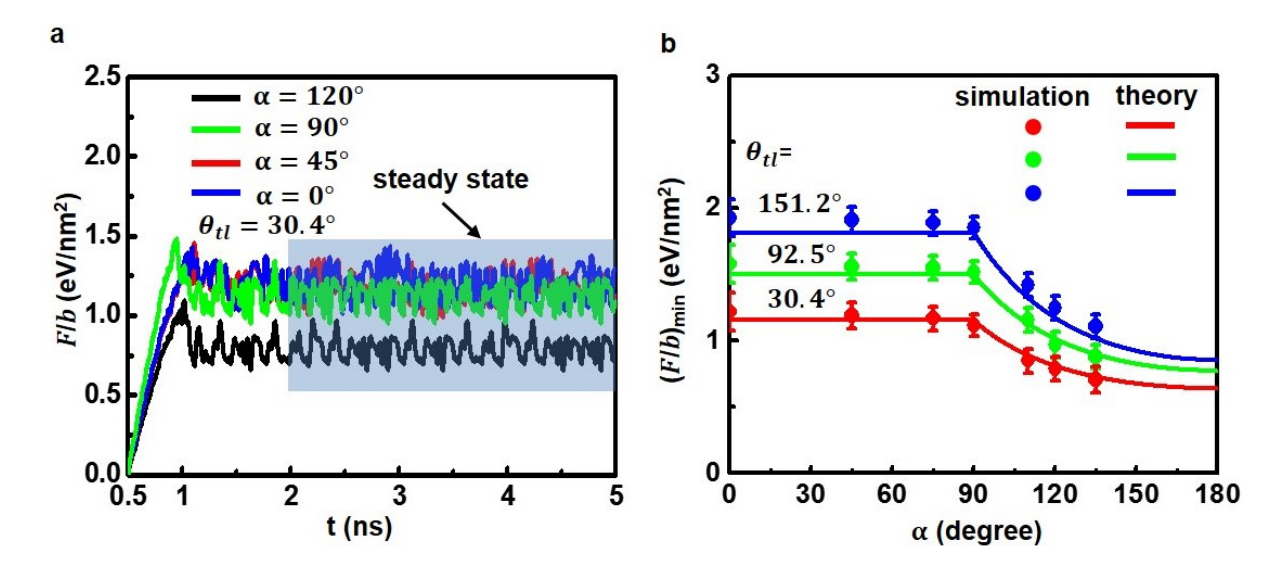


Figure 4. Effect of peeling angle on peel-off force. (a) Peel-off force of graphene at different peeling angles, where surface wettability of graphene and substrate in water is $\theta_{tl} = 30.4^{\circ}$ and $\theta_{sl} = 95.0^{\circ}$, respectively. (b) Comparison of the minimum peel-off force between theory and MD simulations for peeling of graphene with different surface wettability θ_{tl} .

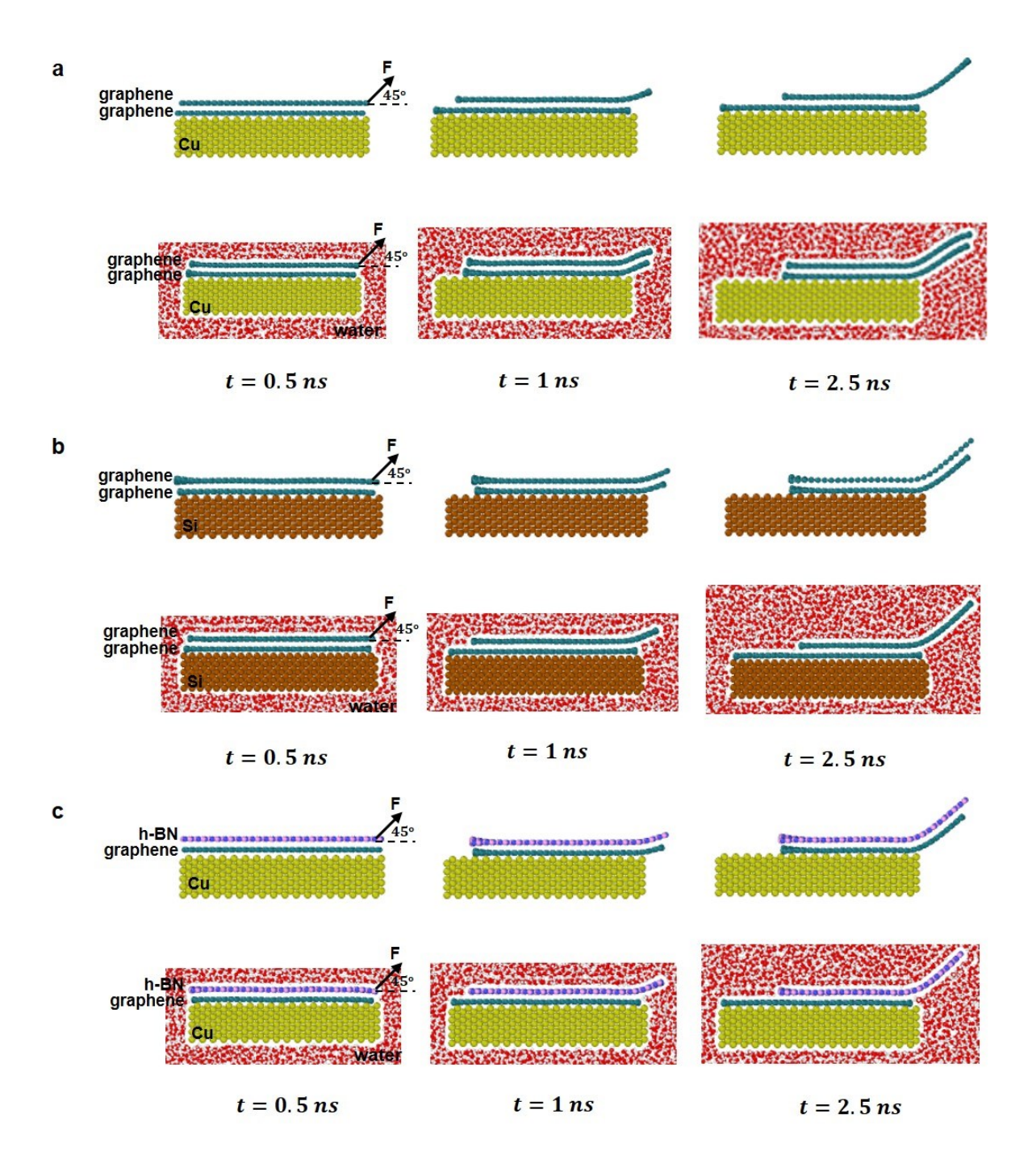


Figure 5. MD simulation of a selective peeling of layer(s) from a substrate in dry and liquid environments. Comparison of the peeling process in dry condition and water environments for the system of (a) graphene/graphene on copper substrate (b) graphene/graphene on silicon (Si) substrate (c) h-BN/graphene on copper (Cu) substrate. The peel-off force is applied on the top layer at a peeling angle $\alpha = 45^{\circ}$.

Supplementary Information

Liquid-Assisted, Etching-Free, Mechanical Peeling of 2D Materials

Yue Zhang, Qingchang liu and Baoxing Xu*

Department of Mechanical and Aerospace Engineering, University of Virginia,

Charlottesville, VA 22904, USA

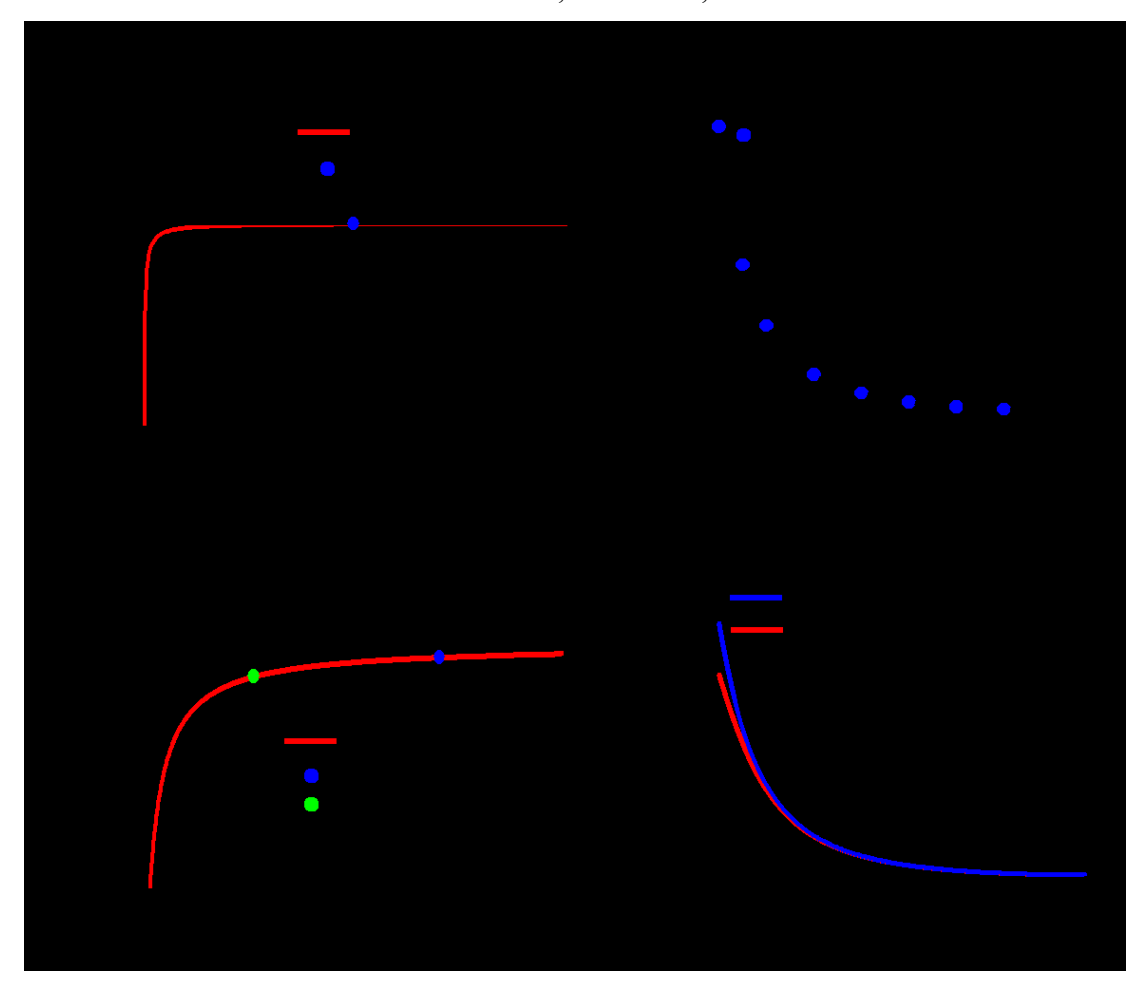


Figure S1. Comparison of peel-off force with and without the elastic deformation of peeled materials in a liquid environment. (a) Peel-off force versus elastic modulus E of peeled graphene. The peeling angle $\alpha = 90^{\circ}$. (b) Peel-off force of graphene versus peeling angle α . The elastic modulus of graphene E = 1 TPa, the thickness t = 0.34nm, the interlayer adhesion energy $G_{ts} = 1.45 \text{eV}/nm^2$, the surface tension of liquid $\gamma_l = 61.3 \times 10^{-3} N/m$ and the contact angle $\theta_{tl} = \theta_{sl} = 95.0^{\circ}$. (c) Peel-off force versus elastic modulus E of black phosphorene (BP). The peeling angle $\alpha = 90^{\circ}$. (d) Peel-off force of black phosphorene versus peeling angle α . The elastic modulus is E = 41.3 GPa and E = 106.4 GPa for armchair and zigzag black phosphorene, respectively. The thickness t = 0.529nm, the interlayer adhesion energy $G_{ts} = 2.24 \text{eV}/nm^2$, the surface tension of liquid $\gamma_l = 61.3 \times 10^{-3} N/m$ and the contact angle $\theta_{tl} = \theta_{sl} = 90.0^{\circ}$.

-

^{*} Corresponding author: bx4c@virginia.edu

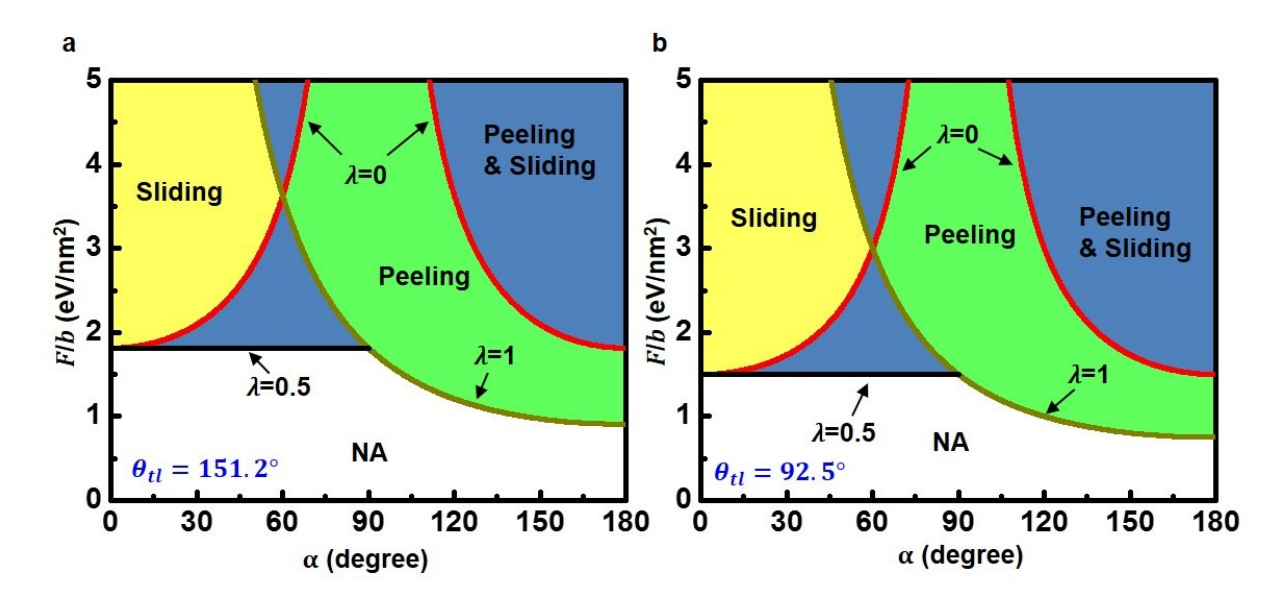


Figure S2. Peel-off force of peeling of a single layer graphene from substrate versus peeling angle α for (a) $\theta_{tl}=151.2^{\circ}$ (b) $\theta_{tl}=92.5^{\circ}$.

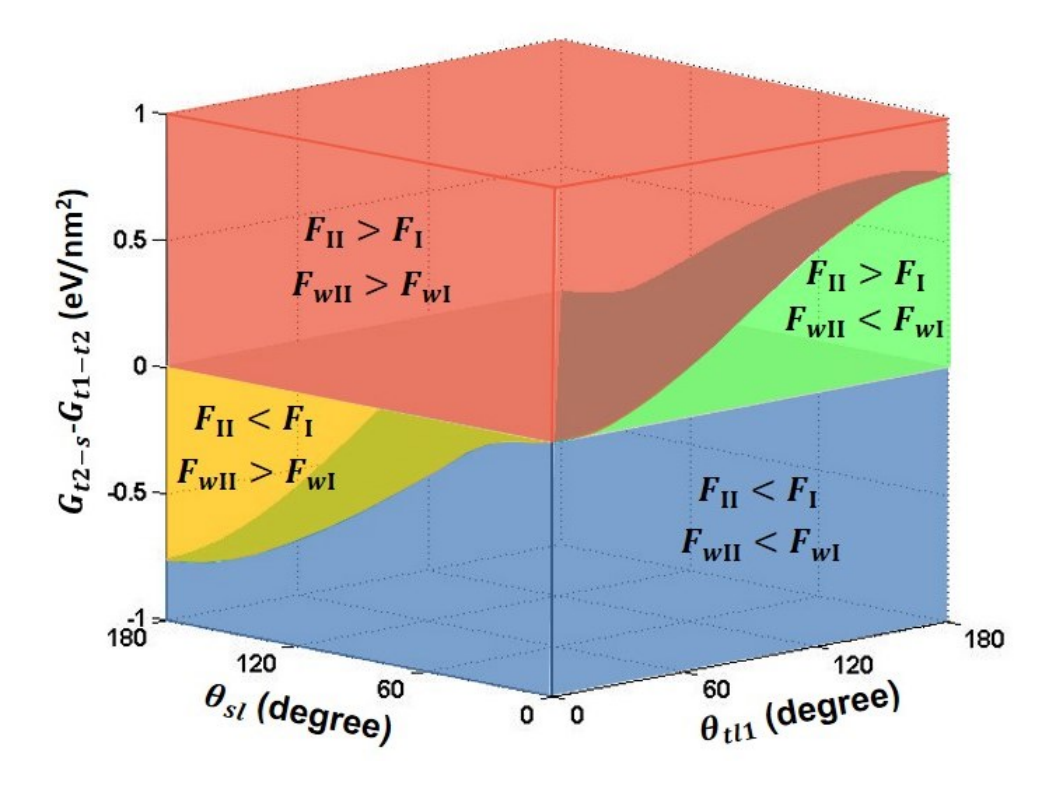


Figure S3. Theoretical map of the peel-off force with variation of surface wettability of substrate θ_{sl} , the top layer thin film θ_{tl1} and adhesion energy difference in dry condition $G_{t2-s}-G_{t1-t2}$.

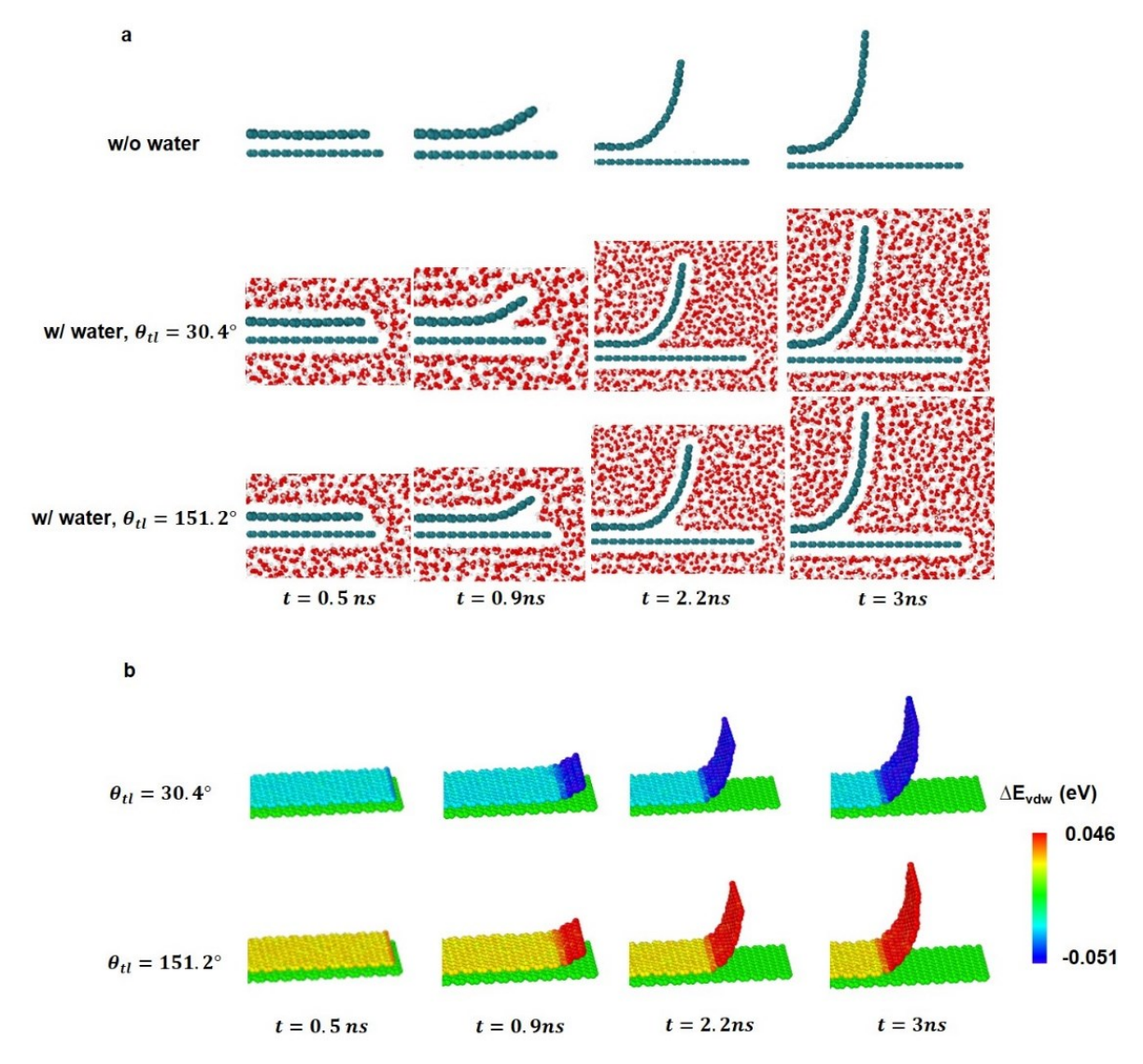


Figure S4. (a) MD simulation snapshots of the peel-off process in dry condition and water environment with $\theta_{tl}=30.4^{\circ}$ and $\theta_{tl}=151.2^{\circ}$. (b) The vdW adhesion energy difference of graphene layer between that in water environment and dry condition for $\theta_{tl}=30.4^{\circ}$ and $\theta_{tl}=151.2^{\circ}$ during the peel-off process.

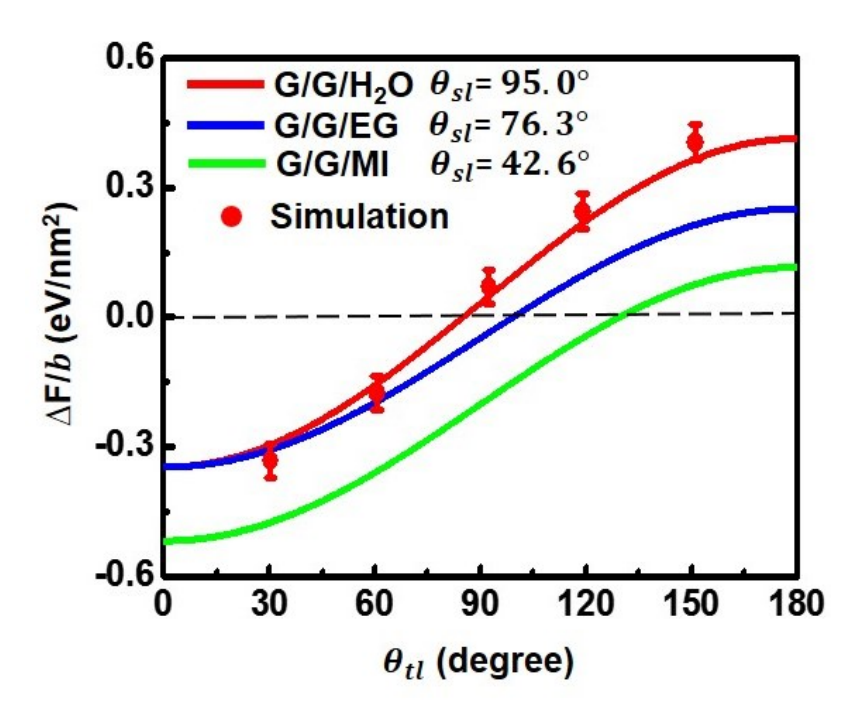


Figure S5. Peel-off force change $\Delta F/b$ at the steady state of peeling of graphene with different surface wettability θ_{tl} in dry condition and in different liquid solvents θ_{sl} (H₂O: water, EG: ethylene glycol, MI: diiodo-methane, G: graphene). The peeling angle $\alpha = 90^{\circ}$.

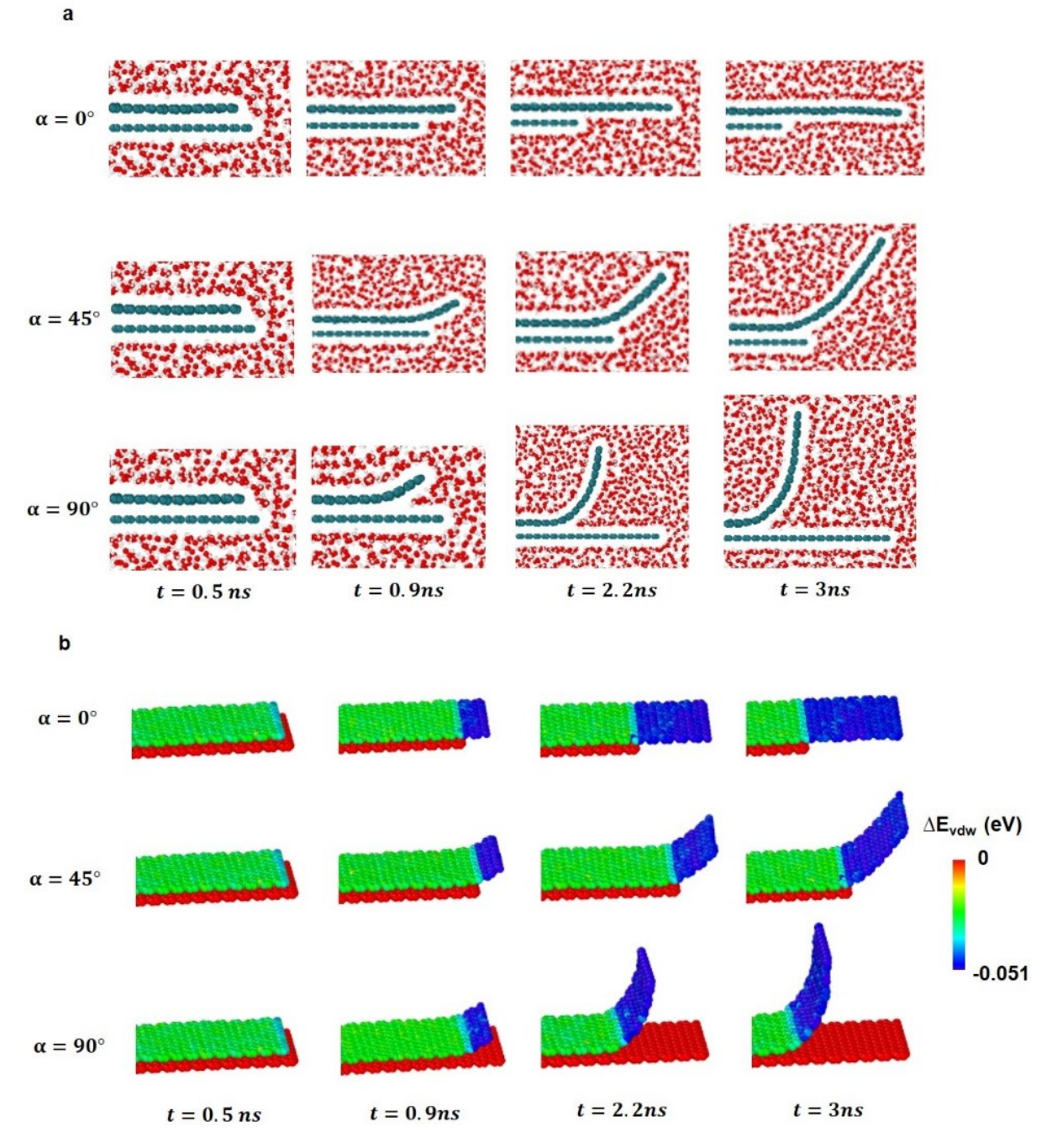


Figure S6. (a) MD simulation snapshots of the peel-off process in water environment with $\theta_{tl} = 30.4^{\circ}$, for peeling angle $\alpha = 0^{\circ}$, $\alpha = 45^{\circ}$ and $\alpha = 90^{\circ}$. (b) The vdW adhesion energy difference of graphene layer with $\theta_{tl} = 30.4^{\circ}$ between that in water environment and dry condition, for peeling angle $\alpha = 0^{\circ}$, $\alpha = 45^{\circ}$ and $\alpha = 90^{\circ}$ during the peel-off process.

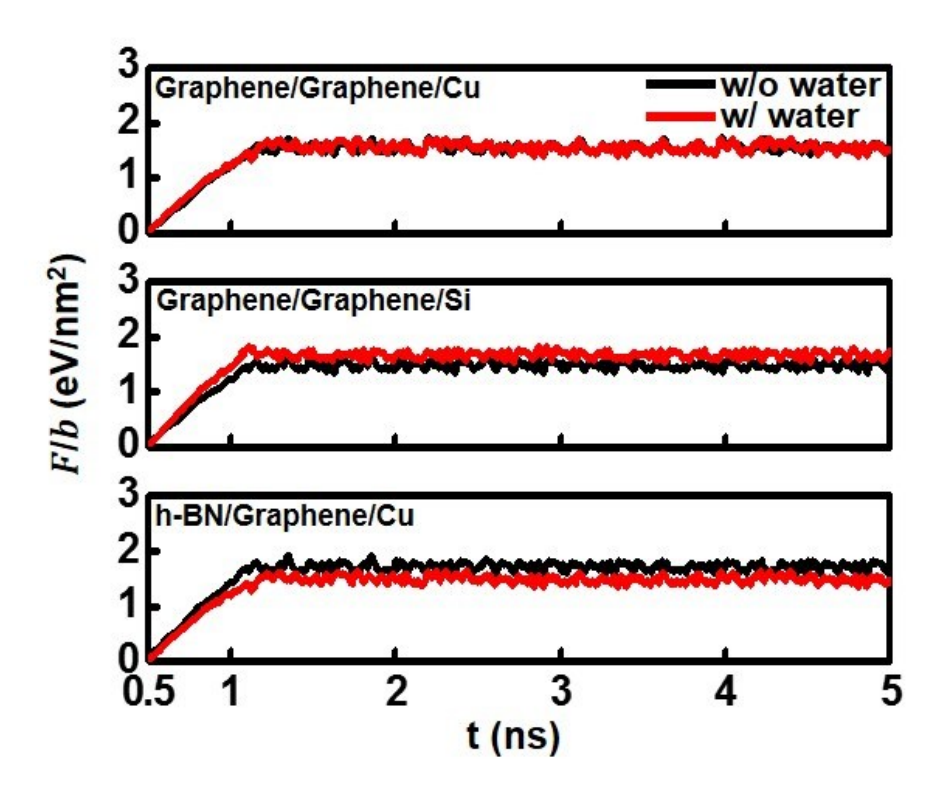


Figure S7. Comparison of peel-off force for the system of graphene/ graphene on copper substrate, graphene/graphene on silicon substrate, and h-BN/graphene on copper substrate in water environment and dry condition.